Icarus 396 (2023) 115499

Contents lists available at ScienceDirect

Icarus

journal homepage: www.elsevier.com/locate/icarus

Infrared spectra and optical constants of astronomical ices: *V*. cyclopropane and ethylene oxide

Reggie L. Hudson [a,*], Perry A. Gerakines [a], Yukiko Y. Yarnall [a,b]

[a] *Astrochemistry Laboratory, NASA Goddard Space Flight Center, Greenbelt, MD 20771, USA*
[b] *Oak Ridge Associate Universities, Greenbelt, MD 20771, USA*

ARTICLE INFO

Keywords:
Ices
IR spectroscopy
TNOs
Titan
Comets
Organic chemistry
Infrared observations

ABSTRACT

Infrared (IR) spectra of solid cyclopropane (*c*-C_3H_6) and ethylene oxide (*c*-C_2H_4O), two cyclic aliphatic compounds, have been recorded in their amorphous and crystalline states. The spectra have been combined with measurements of density and refractive index ($\lambda = 670$ nm) for each form of each solid to compute IR intensities (i.e., absorption coefficients and band strengths) and optical constants for use in laboratory experiments and astronomical observations. These are the first such measurements of absolute IR intensities and optical constants for each solid at temperatures relevant to the outer Solar System and the interstellar medium, with all results coming from a single laboratory. Two literature band strengths for ethylene oxide's strongest IR feature, one value a calculation and the other a gas-phase measurement, need to be increased by ~25% to match the solid-phase value reported here. Suggestions are made for applications and future work related to the chemistry of icy bodies in the Solar System and beyond, including Pluto's surface, Titan's atmosphere, and the formation of cometary C_3.

1. Introduction

Table 1 lists the nine common aliphatic hydrocarbons of three carbons or less. To date we have measured and published the infrared (IR) spectra and IR intensities of the table's first eight entries as hydrocarbon ices, leaving only cyclopropane (*c*-C_3H_6), which we examine in this paper. Fig. 1 shows the structure of a cyclopropane molecule, along with that of ethylene oxide (*c*-C_2H_4O), an epoxide also known as oxirane, which is isoelectronic with cyclopropane and which is also covered in this paper. The pairing of these 18-valence electron, cyclic molecules for IR study goes back many years (Linnnett, 1938; Herzberg, 1945), but solid-phase results of the type presented here have not been published.

Both cyclopropane and ethylene oxide are relevant to planetary and interstellar chemistry. These compounds can be expected to exist as solids in environments such as Pluto's methane-rich regions, cometary ices, the atmosphere of Titan, and the icy mantles of interstellar grains. Gas-phase ethylene oxide is well known as an interstellar molecule (Dickens et al., 1997), and has been identified in Titan atmospheric simulation experiments (Coll et al., 2003). Cyclopropane can be expected to be a reaction product in Titan's atmosphere (Navarro-González and Ramírez, 1997), as a member of the so-called "hydrocarbon zoo" (Nixon et al., 2014), and to condense out as a solid. Its lack of a permanent dipole moment means that cyclopropane is invisible to radio observations, but is detectable by IR methods.

For either telescope- or spacecraft-based IR studies of extraterrestrial solids, such as cyclopropane and ethylene oxide, it is crucial that reference spectra be available. Ideally, such spectra of icy solids are needed at relevant temperatures, and for quantitative work IR spectral intensities are required, most commonly in the form of either band strengths or optical constants. These quantities are reported here for cyclopropane and ethylene oxide, with comparisons to previous work being made in our Discussion section. To anticipate what is there, we simply state that no IR intensity results of the type presented here are in the literature for our two compounds.

Turning to laboratory-based studies, the lack of IR spectral intensities for cyclopropane and ethylene oxide is a hindrance to quantitative studies of both compounds. For example, we have studied the radiolytic formation of many organic and inorganic molecules and ions in icy solids, but we have no accurate yields and reaction rates (e.g., isomerizations) of either cyclopropane or ethylene oxide due to a lack of IR band strengths. Spectra of ethylene oxide have been published by Schriver et al. (2004), but they were measured in a reflection mode and

* Corresponding author at: Astrochemistry Laboratory (Code 691), NASA Goddard Space Flight Center, Greenbelt, MD 20771, USA.
E-mail address: reggie.hudson@nasa.gov (R.L. Hudson).

https://doi.org/10.1016/j.icarus.2023.115499
Received 1 September 2022; Received in revised form 15 February 2023; Accepted 23 February 2023
Available online 3 March 2023
0019-1035/Published by Elsevier Inc.

Table 1
Hydrocarbon ices studied - IR band strengths and optical constants.

Type	Name	Formula	Reference
C_1	methane	CH_4	Gerakines and Hudson (2015a)
C_2	ethane	C_2H_6	Hudson et al. (2014b)
C_2	ethylene	C_2H_4	Hudson et al. (2014b)
C_2	acetylene	C_2H_2	Hudson et al. (2014a)
C_3	propane	C_3H_8	Hudson et al. (2021)
C_3	propylene	C_3H_6	Hudson et al. (2021)
C_3	propyne	C_3H_4	Hudson et al. (2021)
C_3	allene	C_3H_4	Hudson and Yarnall (2022b)
C_3	cyclopropane	c-C_3H_6	

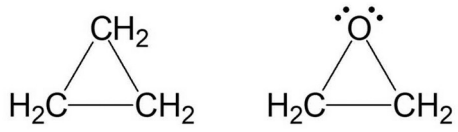

Fig. 1. Two cyclic organic compounds, cyclopropane (left) and ethylene oxide (right). Ethylene oxide is also known as oxirane.

with no sample thicknesses stated. Moreover, the authors specifically mentioned the lack of reference IR intensity data for ethylene oxide. The low-temperature synthesis of ethylene oxide has been examined by Bennett et al. (2005), but to determine reaction yields the authors were forced to use unchecked calculated band strengths in the absence of laboratory data. More recently, Bergner et al. (2019) examined ethylene oxide formation in solids, but adopted a gas-phase band strength near 872 cm^{-1} to determine the reaction's yield, again specifically mentioning the lack of solid-phase data. The papers of Schriver et al. (2004), Bennett et al. (2005), and Bergner et al. (2019) present complex reaction networks and kinetic analyses, but in each case the results for ethylene oxide were somewhat compromised by the lack of band-strength measurements for this compound. In a different type of experiment, Ward and Price (2011) showed that O atoms react with ethylene to make ethylene oxide at temperatures as low as 12 K.

The situation regarding IR band strengths for cyclopropane is, if anything, worse than for ethylene oxide. Ethylene oxide is readily formed through a number of epoxidation pathways, such as the reaction of an O atom with ethylene (C_2H_4, $H_2C{=}CH_2$), and the corresponding O-atom reaction with propylene (C_3H_6, $H_2C{=}CH{-}CH_3$) generates propylene oxide, a chiral interstellar molecule (Hudson et al., 2017a). Since CH_2 (methylene) is isoelectronic with O, it is not surprising that a similar reaction of CH_2 with ethylene produces cyclopropane (e.g., Frey, 1957; DeMore et al., 1959; Doering and Zhao, 1995). Furthermore, since ethylene already is known to be present in Titan's atmosphere (Hesman et al., 2012), and radiolytic formation of CH_2 from CH_4 is known, then cyclopropane production can be confidently predicted. The same hydrocarbon reactants are expected in hydrocarbon-rich regions of Pluto (e.g., Grundy et al., 2016), and so cyclopropane can be predicted there too. However, the lack of solid-phase band strengths for c-C_3H_6 hinders laboratory work on the molecule, including predictions of its abundance on Pluto and other TNOs.

As an aside, we mention the long-standing question of the source of C_3 in cometary comae. Stief, 1972 suggested propyne ($HC \equiv C{-}CH_3$, methyl acetylene) and allene ($H_2C{=}C{=}CH_2$, propadiene) as possible parents, a proposal that was examined in greater detail by Helbert et al. (2005) and Weiler (2012). Related to this suggested source of cometary C_3, Jacox and Milligan (1974) found that UV photolysis of either compound gave rise to C_3, which they identified with both electronic and vibrational spectroscopy. The relevance here is that straightforward reactions starting with cyclopropane can lead to both propyne and allene, a point to which we return later. See also Altwegg et al. (2019) for comments on the C_3 molecule in comets.

As a second aside, we add that Bernstein and Lynch (2009) have suggested that ethylene oxide plays a role in the interstellar medium's unidentified infrared bands (UIRs), so that it is of interest to spectroscopically characterize this molecule.

This paper continues our study of the IR intensities of solid compounds that are either known or suspected to be extraterrestrial. Our goal is still to lessen the dependence on untested IR intensities (e.g., band strengths) by those who study icy solids either in laboratories or with ground- or space-based observatories. Multiple instances in the literature attest to the problems met when IR spectra of ices are analyzed with untested or unchecked gas-phase or computed band strengths. For example, we have found substantial variations between indirect and direct measurements of IR band strengths for ammonia, acetone, acetaldehyde, and HCN ices of 60, 73, 80, and 100%, respectively (Hudson et al., 2022; Hudson et al., 2018; Hudson and Ferrante, 2020; Gerakines et al., 2022). Such differences arising from the application of gas-phase or theoretical IR intensities to the spectra of ices seem to reflect Johnson's statement about the "triumph of wishful thinking over experience" (Boswell, 1791), which we wish to avoid.

2. Laboratory procedures

Essentially all details of our experimental procedures and equipment are in print, and so only a brief summary will be given here. See, for example, Gerakines and Hudson (2015b) or Hudson et al. (2017b) for additional information.

Cyclopropane and ethylene oxide were obtained from Sigma Aldrich (now MilliporeSigma) with stated purities of ≥99%, and used as received. Comparisons with literature spectra confirmed the purity of each reagent. Ices of each compound were made by vapor-phase condensation onto a CsI substrate that was pre-cooled to the temperature of interest, which always was in the 10–120 K range. Interferometry (e.g., Hollenberg and Dows, 1961; Tempelmeyer and Mills, 1968) was used to measure the thickness of each ice, typical growth rates being on the order of an increase in the ice sample's thickness of about 1 μm per hour. An ice's thickness could be measured to, at best, about a tenth of a single interference fringe, which is equivalent to about 0.02 μm. All IR spectra shown are for an ice thickness of ~1 μm.

Refractive indices of our ices were needed to measure ice thicknesses, absorption coefficients, and optical constants, and, in conjunction with ice densities (ρ), to calculate IR band strengths, prime goals of this work. We measured refractive indices (λ = 670 nm) by two-laser interferometry and densities by microbalance gravimetry. See Hudson et al. (2017b) for details concerning the UHV chamber (P ~ 10^{-10} Torr) used for density (ρ) and refractive index (n) determinations. See Luna et al. (2012) for similar measurements from a different research group.

As in our most recent work, a Thermo iS50 spectrometer was used to record IR spectra, each spectrum consisting of 200 accumulations. Tests at several resolutions confirmed that 1 cm^{-1} was sufficient to record all details of interest. The spectral range of greatest interest extended from 5500 to 500 cm^{-1} (1.8 to 20 μm), but a few spectra were recorded at higher wavenumbers (shorter wavelengths) with a near-IR source. Spectra were recorded in a conventional transmission mode with the IR beam perpendicular to the plane of the ice and CsI substrate.

Table 2
Refractive indices and densities of two cyclic compounds.[a]

	Cyclopropane, c-C_3H_6		Ethylene Oxide, c-C_2H_4O	
Form	n	ρ / g cm^{-3}	n	ρ / g cm^{-3}
Amorphous	1.414 (15 K)	0.769 (15 K)	1.348 (15 K)	0.921 (15 K)
Crystalline	1.512 (65 K)	0.916 (65 K)	1.458 (100K)	1.142 (100 K)

[a] Values of n and ρ are averages of at least three measurements; the wavelength for n was 670 nm; uncertainties are ±0.005 for n and ± 0.005 g cm^{-3} for ρ.

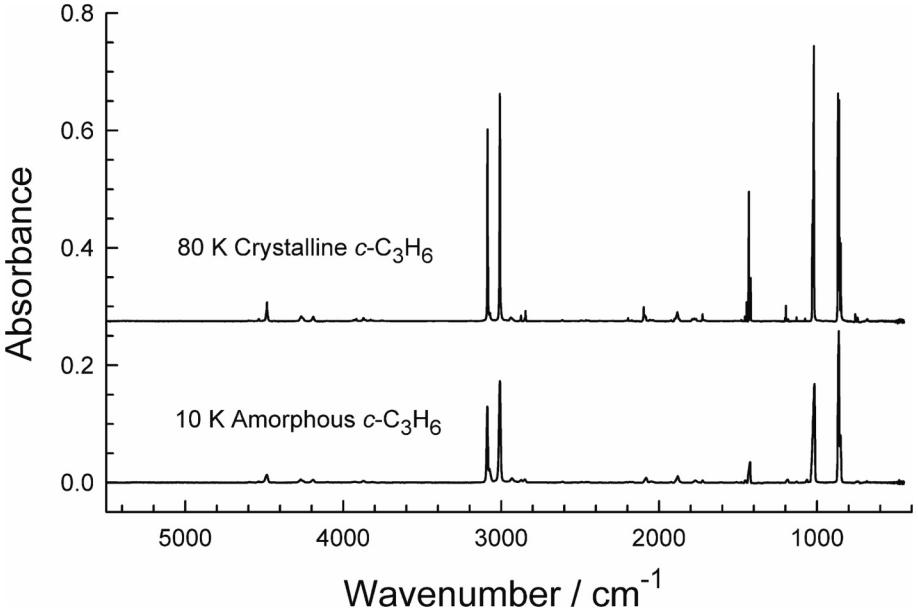

Fig. 2. Survey spectra of cyclopropane deposited at 10 and 80 K. Ice thicknesses were 0.97 ± 0.02 and 0.94 ± 0.02 μm at 10 and 80 K, respectively.

The minimum temperature of the cryostat used for our IR work varied during the course of these experiments from about 8 to about 12 K. For convenience, we simply state the lowest temperature as 10 K. The base vacuum pressure at room temperature was on the order of 10^{-8} Torr for IR work and 10^{-10} Torr for measurements under UHV conditions (densities and refractive indices).

3. Results

3.1. Densities and refractive indices

The refractive indices and densities and used in this work are listed in Table 2, with uncertainties (standard errors) of ±0.005 and ± 0.005 g cm^{-3}, respectively, based on a minimum of three measurements in each case. These values were reported previously for the amorphous ices in Hudson et al. (2020) and in Yarnall and Hudson (2022a) for the crystalline solids. No comparison data for the amorphous ices has been found, but our crystalline ices' densities compare favorably to those measured in diffraction studies (Yarnall and Hudson, 2022a). We note that n and ρ for the two amorphous ices in Table 2 are smaller than the corresponding values for crystalline solids, a trend we have seen for other compounds. As in Hudson et al. (2017b) our measurements of n involve two-laser interferometry in which laser angles are known to three significant figures at best. An extra significant figure has been carried for some entries of Table 2 and elsewhere, but rounding can be done as desired.

Our values of n and ρ can be used to estimate the polarizabilities (α) of cyclopropane and ethylene oxide from

$$(4\pi/3)\, N_A\, \alpha = (M/\rho)\, \left(n^2 - 1\right)/\left(n^2 + 2\right) \quad (1)$$

where N_A is Avogadro's constant and M is molar mass (Born and Wolf, 1964; Kragh, 2018). The results are 5.44 and 4.12 Å^3 for cyclopropane and ethylene oxide, respectively, in reasonable agreement with, and in the correct order for, the measured values of 5.52 and 4.32 Å^3 in Thakkar and Wu (2015).

3.2. Cyclopropane – IR spectra

Two survey spectra of cyclopropane are shown in Fig. 2 for ices made by vapor-phase deposition onto a CsI substrate. The lower trace is for a 10-K deposition to make the amorphous form of the compound. The upper trace is for an 80-K deposition to make crystalline cyclopropane. Channel fringes have been removed from the two spectra, and both show good signal-to-noise ratios and little if any contamination. Such spectra are useful as quick summaries of peak positions and relative intensities.

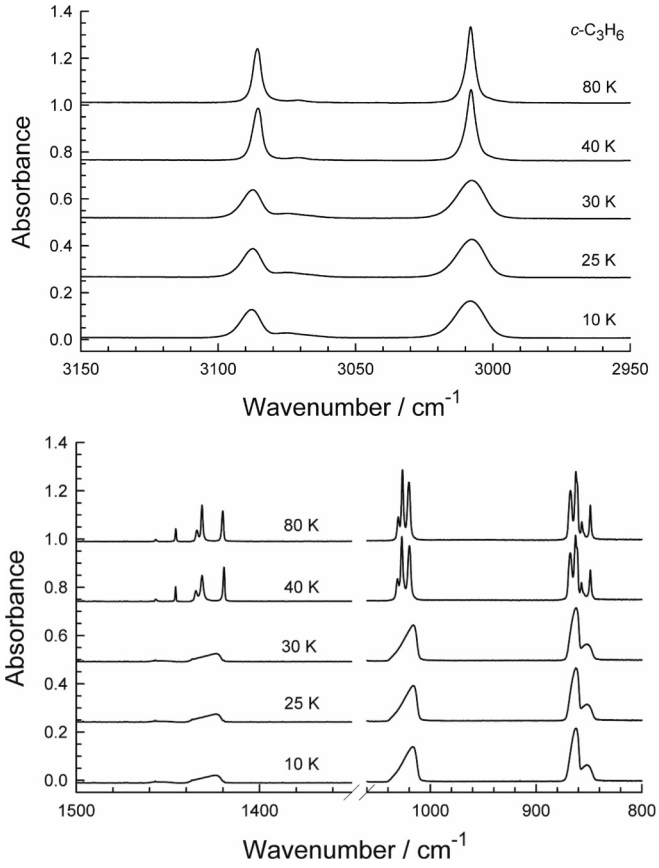

Fig. 3. Cyclopropane deposited at 10 K and warmed to 25, 30, 40, and 80 K. Spectra are offset vertically by about 0.25. The thickness of the ice at 10 K was 0.88 ± 0.02 μm.

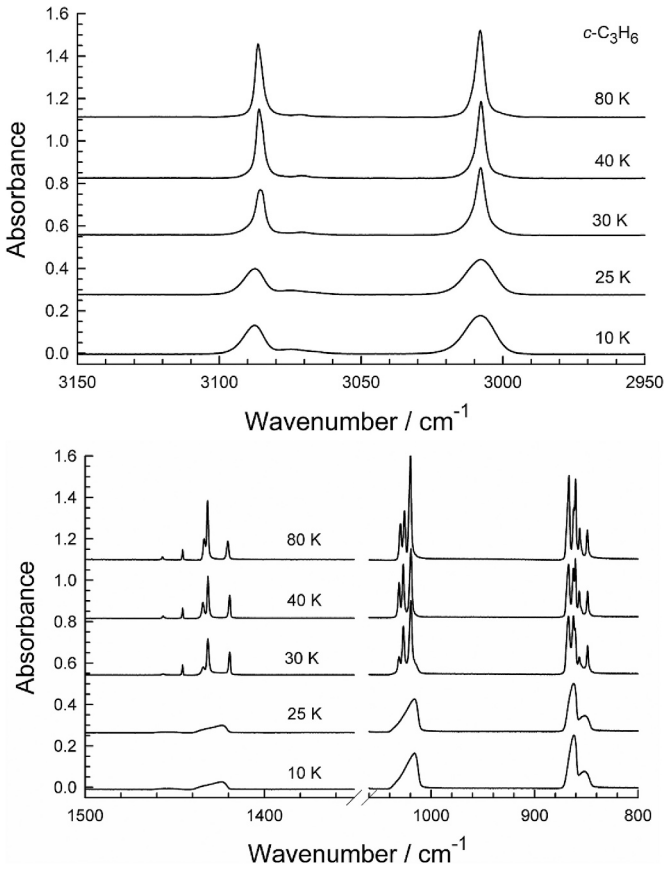

Fig. 4. Cyclopropane deposited at 10, 25, 30, 40, and 80 K. Spectra are offset vertically by about 0.25. The thickness of the ice at 10 K was 1.01 ± 0.02 μm.

Table 3
Infrared peaks of cyclopropane ices.

Vibrational Mode[a]	Amorphous-Ice Position (cm^{-1})[b]	Crystalline-Ice Position (cm^{-1})[b]	Crystalline-Ice Position, Lit. (cm^{-1})[c]
ν_6	3088	3086	3086
ν_{12}	3075	3071	3071
ν_1	3008	3008	3008
ν_8	3008	–	–
ν_2	1454	1457/1446	1457/1446
ν_9	1424	1433/1432/1420	1436/1432/1420
ν_{13}	1186	1201/1197	1201/1196
ν_3	1186	1189/1184/1182	1189/1184/1182
ν_4	1129	1129	1129
ν_5	1064	1076	1076
ν_{10}	1016	1030/1026/1020	1030/1026/1020
ν_{11}	862	867/862/860	867/862/860
ν_7	852	856/849	856/849
ν_{14}	743	758/755/741	758/755/741

[a] The numbering of the vibrations follows that of Shimanouchi (1972) and the NIST Chemistry WebBook entry on cyclopropane.
[b] The amorphous and crystalline ices for this work were grown, and their spectra were recorded, at 10 and 80 K, respectively.
[c] The literature results for crystalline cyclopropane are from the table of Duncan and McKean (1968) for an ice at 78 K.

Fig. 3 shows expansions of the IR spectrum of a cyclopropane ice that was made at 10 K and then warmed to 25, 30, 40, and 80 K. The transition between 30 and 40 K from the rounded features of the amorphous ice to the sharper features of the crystalline ice is clear. All such crystallizations were irreversible. Continued warming gave rise to rapid sublimation of the cyclopropane ice at 100 K, and so the spectra shown here were recorded at 80 K and lower to prevent sample loss. In agreement with Ruehrwein and Powell (1946), we found no evidence for any crystalline-crystalline phase changes for solid cyclopropane in the temperature range of our measurements.

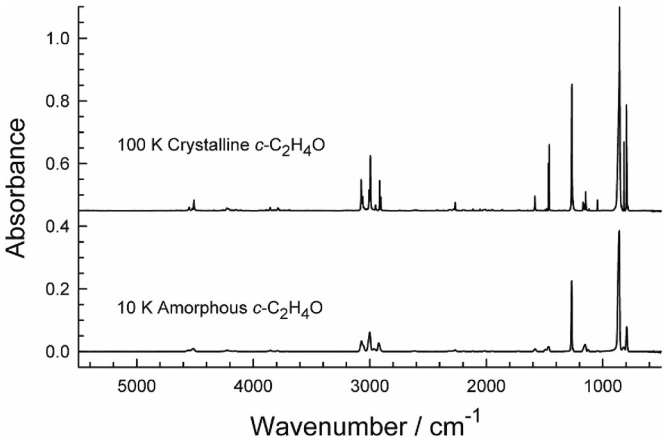

Fig. 5. Survey spectra of ethylene oxide deposited at 10 and 100 K. Ice thicknesses were 1.03 ± 0.02 and 1.00 ± 0.02 μm at 10 and 100 K, respectively.

Fig. 4 shows the result of depositing cyclopropane vapor onto our CsI substrate pre-cooled to 10, 25, 30, 40, and 80 K. The spectra in Fig. 4 of the two ices made at 10 and 25 K are essentially the same as those in Fig. 3 for an ice made at and warmed from 10 K. However, differences can be seen at higher temperatures, especially at 30 K. The ice made at 30 K for Fig. 4 was crystalline, but the ice warmed from 10 to 30 K for Fig. 3 was amorphous. This difference is not surprising, as we have documented multiple cases in which an ice can be crystallized by vapor-phase deposition at a sufficiently high rate and temperature. See our work on other hydrocarbons, such as CH_4 and C_2H_2 (Gerakines and Hudson, 2015a; Hudson et al., 2014a) or on CO_2 and N_2O (Gerakines and Hudson, 2015b; Hudson et al., 2017b). This "self-annealing" of an ice is due to the energy released by condensation of the room-temperature vapor, an observation also made by others (e.g., Jacox, 1962).

Table 3 gives wavenumbers for the fundamental vibrations of cyclopropane in amorphous and crystalline forms. Positions of crystalline cyclopropane also have been published by, for example, Keeports and Eggers (1986) and Bates et al. (1969), and our results agree with theirs. Gas-phase positions from IR and Raman results have been compiled by Shimanouchi (1972).

3.3. Ethylene oxide – IR spectra

Our work with ethylene oxide followed the same sequence used for cyclopropane. Two survey spectra of ethylene oxide are shown in Fig. 5 for ices made by vapor-phase deposition onto a CsI substrate. The lower trace is for a 10-K deposition to make the amorphous form of the compound. The upper trace is for a 100-K deposition to make crystalline ethylene oxide. As with our cyclopropane spectra, channel fringes have been removed from the spectra of Fig. 5, and both show good signal-to-noise ratios with little if any contamination.

Fig. 6 shows the spectrum of an amorphous ethylene oxide ice made at 10 K. Few changes were seen on warming to about 70 K, but above that temperature the IR bands sharpened considerably, as shown for the 75-K spectrum in the figure. Additional warming gave a second set of changes, as seen in the 100-K spectrum. Above about 110 K, the ice underwent rapid sublimation with no apparent changes in the shapes or relative intensities of the IR features. Ices made by depositing ethylene oxide at 70 and 100 K gave spectra similar to those of ices warmed from 10 K. As with cyclopropane, the changes seen on warming to crystallize

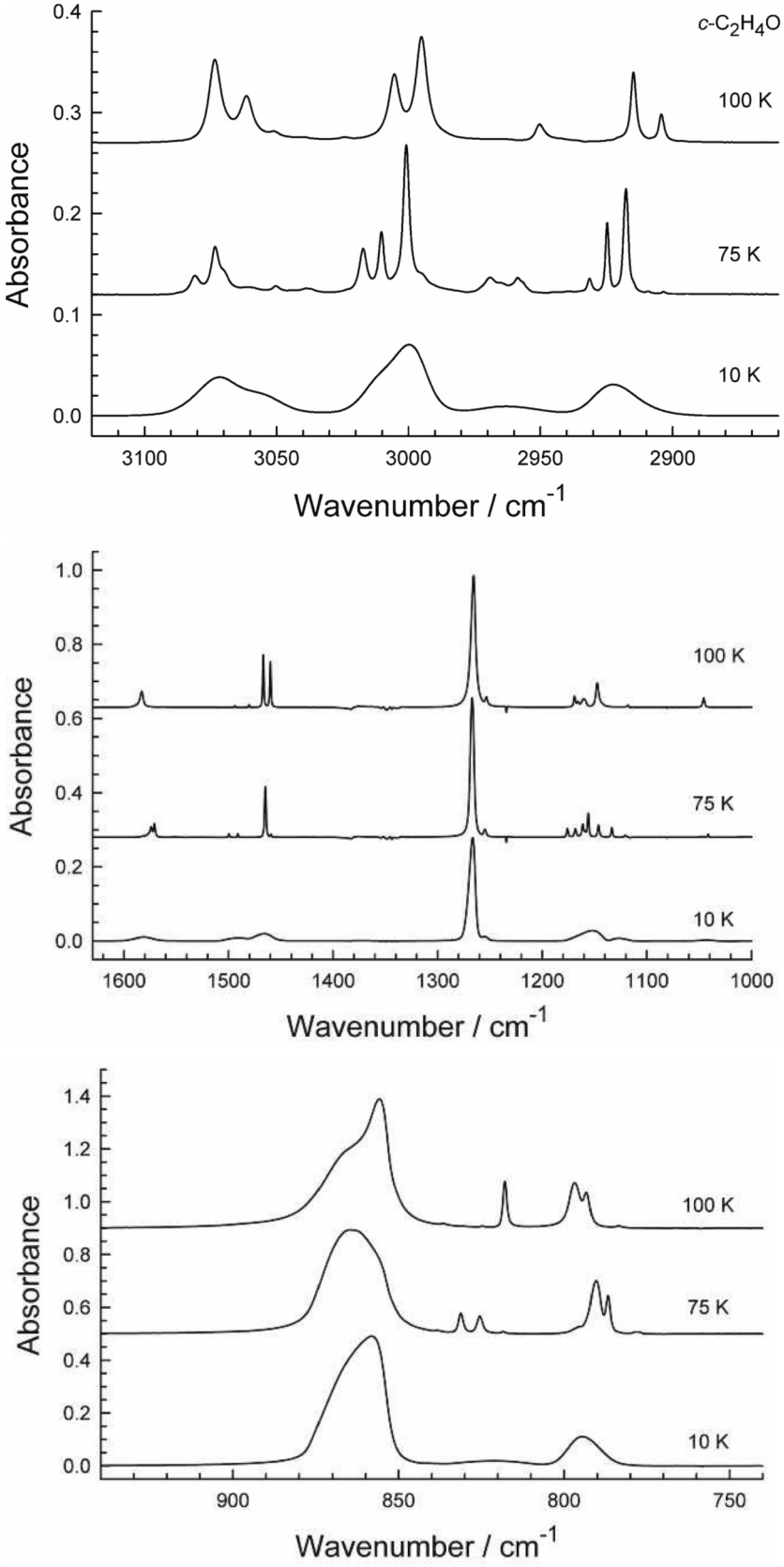

Fig. 6. Expansions of the IR spectrum of ethylene oxide that was made at 10 K and warmed to 75 and 100 K. The thickness of the ice at 10 K was 1.25 ± 0.02 μm.

Table 4
Infrared peaks of ethylene oxide ices.

Vibrational Mode[a]	Amorphous-Ice Position (cm^{-1})[b]	Crystalline-Ice Position (cm^{-1})[b]	Crystalline-Ice Position, Lit. (cm^{-1})[c]
ν_{13}	3072	3073	3074
ν_6	3058(sh)	3061	3062
ν_1	3010(sh)	3005	3006
ν_9	3000	2995	2996
ν_2	1491	1494/1480	1495/1481
ν_{10}	1466	1467/1460	1467/1460
ν_3	1266	1265	1266
ν_{11}	1152	1170/1166	1170/1167
ν_{14}	[d]	1160/1147	1161/1147
ν_4	1127	1118	1119
ν_7	1042	1046	1046
ν_5	858	865(sh)/855	875(sh)/859
ν_8	[d]	837	837
ν_{12}	821	825/818	825/818
ν_{15}	795	796/793/783	798/794/784

[a] The numbering of the vibrations follows that of Bertie and Jacobs (1978).
[b] The amorphous and crystalline ices for this work were grown, and their spectra were recorded, at 10 and 100 K, respectively. sh = shoulder.
[c] The literature results for crystalline ethylene oxide at 100 K are from the compilation of Bertie and Jacobs (1978). sh = shoulder.
[d] Unresolved feature in the spectrum of amorphous ethylene oxide.

the ice were irreversible (i.e., lowering the temperature from 100 K to 75 K and then 10 K did not regenerate the spectra at 75 K and 10 K of Fig. 6).

The most striking spectral difference between cyclopropane and ethylene oxide ices was that the latter showed, in Fig. 6, evidence of two crystalline forms, one appearing near 75 K, the other near 100 K. The one near 75 K was metastable in the sense that it always converted into the form seen at 100 K, but the reverse never took place. We also found that of the ices studied in this work, the metastable one seen on warming amorphous ethylene oxide to 75 K was formed only by that procedure. Depositions at 75 K inevitably gave either a mixture of the two crystalline forms or only the form seen at 100 K. Both rapid (~10 μm / hr) and slow (~0.5 μm / hr) deposition rates were tried in an effort to make the metastable form by direct deposition (i.e., no additional warming), but without success.

Table 4 gives positions of the fundamental vibrations of amorphous and crystalline ethylene oxide, taken from transmission spectra in both cases. We have not found such a comparison in the literature. Positions of crystalline ethylene oxide also have been published by, for example, Cant and Armstead (1975) and our results agree with theirs. See Schriver et al. (2004) for IR peak positions based on reflection measurements.

3.4. Near-IR spectra

Recognizing that the near-IR region ($\tilde{\nu} > \sim 4000\ cm^{-1}$, $\lambda < \sim 2.5\ \mu m$) is important for Solar System observations, in Fig. 7 we show an enlargement of our spectra from 6500 to 3700 cm^{-1} (1.54–2.70 μm), with features for both the amorphous and crystalline forms of cyclopropane and ethylene oxide. The strongest peak in each case is near 4500 cm^{-1} (2.22 μm).

3.5. IR intensities and optical constants

The primary goal of the present work was not to produce yet more tables of peak positions, but rather to measure the intrinsic intensities of selected IR features of solid cyclopropane and solid ethylene oxide in both amorphous and crystalline forms. We were particularly interested in measuring the intensities of the stronger IR bands as they are the ones that are most likely to be useful to laboratory scientists and astronomical observers. In this regard, we intentionally have avoided generating multiple lists of IR positions and vibrational assignments of combinations and overtones that are already in the literature.

To measure IR intensities, we followed the procedures used in our recent papers (e.g., Hudson and Yarnall, 2022a; Hudson and Yarnall, 2022b). Specifically, we made ice samples having a range of thicknesses for both of our compounds and recorded the IR spectrum of each. For each IR peak of interest, a graph of the peak's absorbance as a function of ice thickness (h) was prepared with reference to Eq. (2) below. Such graphs were linear with slopes that gave apparent absorption coefficients (α'). Integrating IR absorbance bands of the same spectra, and graphing the resulting band areas as a function of thickness according to Eq. (3) below, gave linear plots with slopes from which apparent band strengths (A') were found.

$$Absorbance = \left(\frac{\alpha'}{2.303}\right) h \quad (2)$$

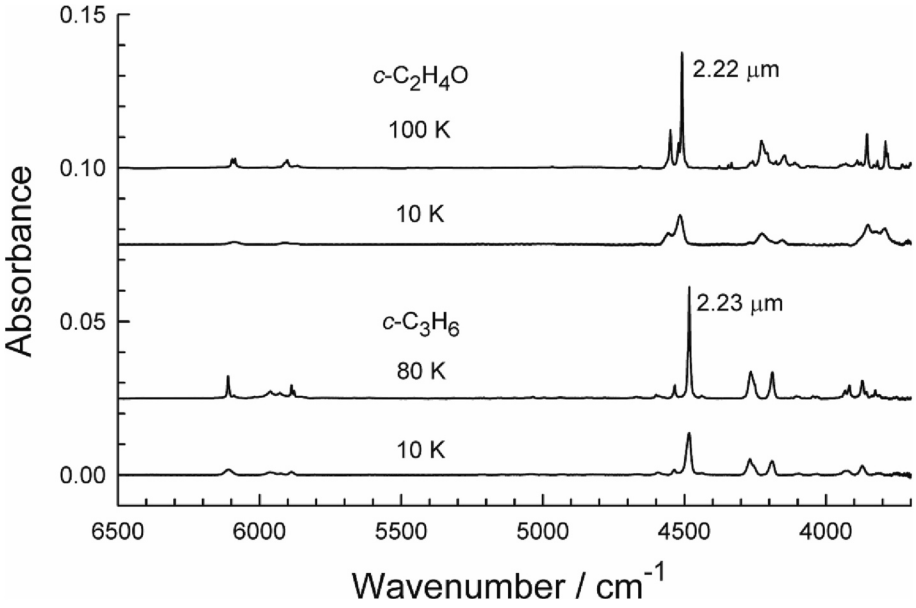

Fig. 7. Near-IR spectra of amorphous and crystalline cyclopropane (c-C_3H_6) and ethylene oxide (c-C_2H_4O). Each spectrum has been scaled to correspond to an ice thickness of 1 μm.

Table 5
Positions and intensities of selected IR features of cyclopropane ices.

Form	$\tilde{\nu}$ / cm^{-1}	α' / cm^{-1}	Integration range / cm^{-1}	A' / 10^{-18} cm molecule^{-1}
Amorphous 10 K	4483	314	4516–4460	0.534
	3088	3000	3110–3050	3.19
	3008	4010	3050–2985	4.97
	1424	871	1442–1400	0.996
	1016	3920	1042–980	5.74
	862	5930	880–820	6.78
	852	1900		
Crystalline 80 K	4483	829	4500–4460	0.545
	3086	9150	3103–3050	3.07
	3008	10,500	3025–2985	3.91
	1432	5130	1438–1425	0.885
	1020	11,100	1040–1000	4.73
	867	9900	875–840	5.87
	860	8950		

Table 6
Positions and intensities of selected IR features of ethylene oxide ices.

Form	$\tilde{\nu}$ / cm^{-1}	α' / cm^{-1}	Integration range / cm^{-1}	A' / 10^{-18} cm molecule^{-1}
Amorphous 10 K	4515	217	4600–4450	0.751
	3072	683	3120–3032	1.40
	3000	1270	3032–2980	1.91
	1466	369	1520–1440	0.800
	1266	5189	1285–1245	3.37
	858	9040	950–836	13.4
	795	2110	806–775	1.85
Crystalline 100 K	4508	856	4600–4450	0.740
	3073	2550	3100–3032	1.64
	2995	4090	3032–2958	2.14
	1467	3810	1470–1450	0.719
	1460	4310		
	1265	9330	1290–1220	3.81
	855	14,600	920–822	14.1
	818	5216	822–808	0.498
	796	6940	808–767	2.29

$$\int_{band} (Absorbance)\, d\tilde{\nu} = \left(\frac{\rho_N A'}{2.303}\right) h \quad (3)$$

Note that the factor of ln(10) ≈ 2.303 in eqs. (2) and (3) was needed to convert absorbance to optical depth, and that ρ_N is the number density (molecules cm^{-3}) of the ice, computed from our measured densities in Table 2 as $\rho_N = \rho\ (N_A / M)$ where, again, M is molar mass of the compound and N_A is Avogadro's constant. Additional details are in Hudson et al. (2021). All plots prepared according to eqs. (2) and (3) had correlation coefficients of 0.99 and higher.

Tables 5 and 6 list the α' and A' values that we determined for amorphous and crystalline cyclopropane and ethylene oxide. These are the first such intensity measurements for these two solid compounds. Uncertainties in α' and A' were estimated as in our recent paper on allene (Hudson and Yarnall, 2022b) by using both a propagation-of-error approach and a linear least-squares fitting routine that considers uncertainties in both the x and y quantities of Beer's law plots corresponding to eqs. (2) and (3). See Irvin and Quickenden (1983) and Press et al. (1992) for mathematical details. Uncertainties in α' and A' were near 2% for mid-IR features ($\tilde{\nu} \leq 4000$ cm^{-1}) of amorphous ices, rising to about 3 and 7% for α' and A', respectively, for near-IR absorbances ($\tilde{\nu} >$ 4000 cm^{-1}). Uncertainties in α' and A' were about 4% for mid-IR features of crystalline ices and about 7 and 11%, respectively, for near-IR absorbances.

Table 7 gives absorption coefficients for a few of the near-IR features we observed near 6000 cm^{-1}. No other work was done with these peaks due to their weakness and the fact that they reside in a region of strong H_2O-ice features, hindering astronomical observation (e.g., Roush, 2001).

Table 7
Positions and intensities of selected near-IR features of ethylene oxide and cyclopropane ices.

Compound	T / K	Form	Position of Peak / cm^{-1}	α' / cm^{-1}
ethylene oxide	100	crystalline	6097	66
ethylene oxide	100	crystalline	6087	68
ethylene oxide	10	amorphous	6090	19
cyclopropane	80	crystalline	6111	162
cyclopropane	10	amorphous	6110	40

The IR features used for intensity measurements were chosen to cover different regions across the spectra of c-C_3H_6 and c-C_2H_4O ices, focusing on the stronger absorbances. Although it was relatively straightforward to select and measure peak heights and α', measuring areas and A' was complicated by overlapping IR features. In such cases, we decided not to separate band areas, preferring to let each user decide on baseline adjustments, line-shape assumptions, and curve fitting routines to deconvolve overlapping IR bands.

Band strengths and absorption coefficients are valuable indicators of IR intensities, and from them molecular abundances can be determined. However, some astronomers use optical constants to calculate spectra that match those of extraterrestrial surfaces. Therefore, having spectra of cyclopropane and ethylene oxide in hand, we used them to calculate the two components, $n(\tilde{\nu})$ and $k(\tilde{\nu})$, of the complex refractive index, $n(\tilde{\nu})$ - $ik(\tilde{\nu})$, of each compound from 5500 to 500 cm^{-1}. The calculation has been described in detail in Gerakines and Hudson (2020), to which interested readers are referred. The implementation of the procedure described there is available in two different versions, one in Python and the other as a Windows executable file. We emphasize that this remains the only such open-source software freely available to the scientific community. Tests of its accuracy and speed, and comparisons to other software, are given in Gerakines and Hudson (2020). We strongly encourage the use of open software for all such calculations, and their publication, as opposed to the use of proprietary, unshared, or otherwise hidden computer routines that cannot be independently tested.

Figs. 8 and 9 show the optical constants we calculated for amorphous and crystalline cyclopropane and ethylene oxide at the temperatures indicated in the figures. The calculations were done up to 5000 cm^{-1}, but results above 3400 cm^{-1}, are not shown as they would be too small to be readily seen on the scale of these figures. All optical constants are available on our group's website at https://science.gsfc.nasa.gov/691/cosmicice/constants.html, along with our software.

4. Discussion

4.1. IR spectra

We have not found IR transmission spectra of either amorphous cyclopropane or amorphous ethylene oxide for comparison to the spectra in our figures. However, to the extent that amorphous solids resemble frozen liquids then we can say that our spectra are in qualitative agreement with those published by Brecher et al. (1961); Fig. 1) for liquid cyclopropane and by Bertie and Othen (1973); Fig. 2) for liquid ethylene oxide in terms of the IR peaks present, their positions, and their relative intensities. Little more can be said due to the size of the published figures and the lack of sample thicknesses in the older work.

The situation is only slightly better for our crystalline ices. Bates et al. (1969) published segments of the IR spectrum of crystalline cyclopropane at 85 K, but the relevant figure shows only selected regions and there are no numbers along the vertical axis. The tabulated peak positions, from a dispersive spectrometer, are close (within 1–2 cm^{-1}) to those in our Table 5. In contrast, the peak positions tabulated by

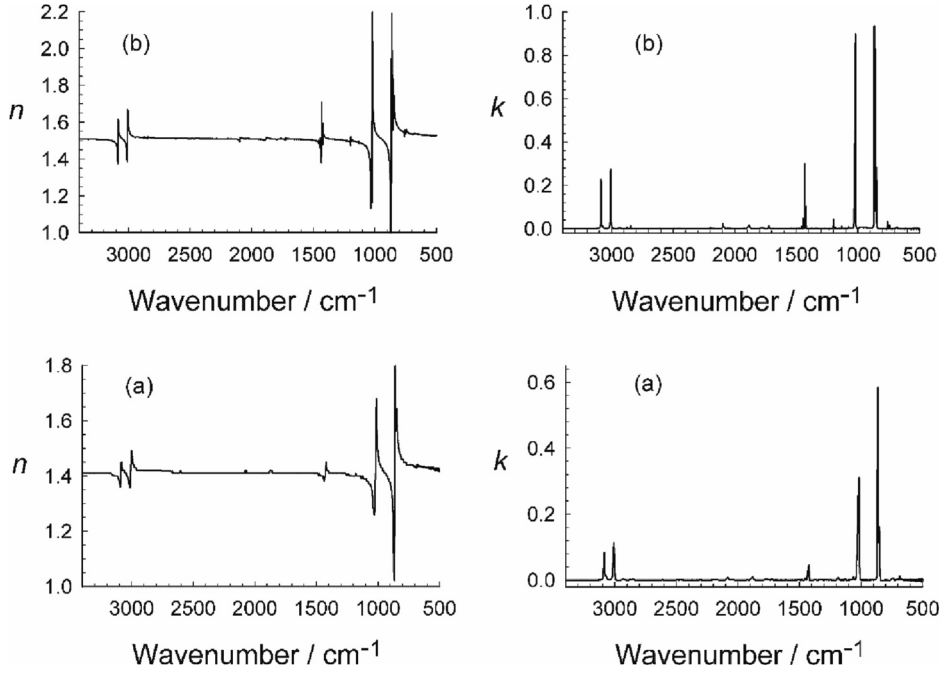

Fig. 8. Mid-IR optical constants of (a) amorphous and (b) crystalline cyclopropane (*c*-C_3H_6) at 10 and 80 K, respectively.

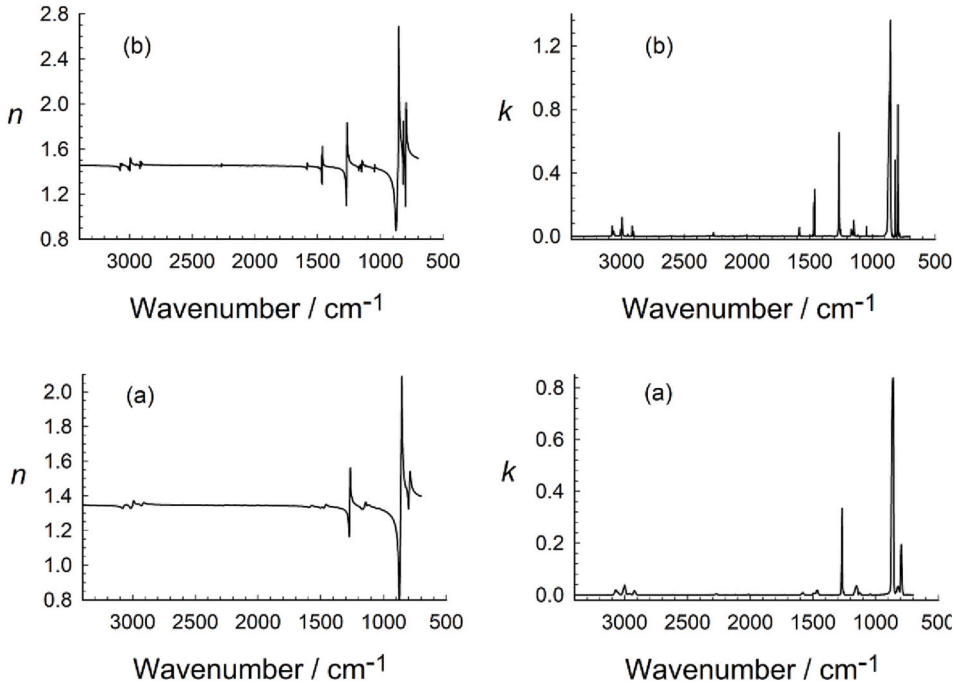

Fig. 9. Mid-IR optical constants of (a) amorphous and (b) crystalline ethylene oxide (*c*-C_2H_4O) at 10 and 100 K, respectively.

Keeports and Eggers (1986) for cyclopropane at 77 K, based on a Fourier transform spectrometer, are in near-exact agreement with ours, but intensity comparisons cannot be made as no spectrum was shown.

Crystalline ethylene oxide has been the subject of several studies, but again spectra that can be compared to our work are hard to find. Cant and Armstead (1975) published segments of a spectrum of crystalline ethylene oxide at 77 K, but again without numbers along the vertical axis of their figures. The tabulated peak positions are close (within 1–2 cm^{-1}) to those in our Table 6. Cataliotti and Paliani (1982) published one figure showing only two segments of the IR spectrum of crystalline ethylene oxide, and lacking numbers along the vertical axis. The tabulated peak positions are close to ours, but little more can be said.

Special mention should be made here of a study of amorphous and crystalline ethylene oxide by Schriver et al. (2004). Those authors documented spectral changes with temperature just as we have, and our results agree with theirs in terms of spectral changes and IR peak positions. However, no details were provided by the authors about how ice thicknesses were determined, and specific thicknesses were not given for the ice samples whose spectra were shown, hindering quantitative comparisons. In addition, spectra were recorded in a reflection mode, which can add to sensitivity, but can distort the relative intensities of various IR features (Pacansky and England, 1986). For example, the

Table 8
IR intensities of cyclopropane in the gas phase and as an amorphous ice.

c-C_3H_6 - Gas [a]		*c*-C_3H_6 - Amorphous Ice [b]		
Position/ cm^{-1}	A' / 10^{-18} cm $molecule^{-1}$	Position/ cm^{-1}	A' / 10^{-18} cm $molecule^{-1}$	% Change, Gas to Ice
3102	4.67	3088	3.19	−32
3024	6.96	3008	4.97	−29
1438	0.34	1424	1.00	190
1028	3.57	1016	5.74	61
869 & 854	5.55	862 & 852	6.78	22

[a] Kondo et al. (1979).
[b] This work. See Table 5 and the text for details.

ratio of the heights of those authors' IR bands for amorphous ethylene oxide near 858 and 797 cm^{-1} is about 2.5, compared to the value of about 4.3 from our transmission spectra.

To summarize, the IR spectra we recorded at the lowest and highest temperatures indicated in our figures are in qualitative agreement with literature results. Unfortunately, quantitative comparisons are impossible due to the lack of vertical scales, ice thicknesses, or transmission measurements in published work.

4.2. Two crystalline phases of ethylene oxide?

The warming sequence seen in Fig. 6 at 75 K for ethylene oxide is intriguing. The transition from the rounded peaks of the amorphous solid to the much sharper ones at 75 K suggests that a crystallization took place, which was followed by a second crystallization near 100 K. This situation resembles that met with some other low-temperature ices we have studied with IR spectroscopy. For example, amorphous methanethiol (CH_3SH) crystallized on warming into the compound's high-temperature phase, but on standing or with additional warming we observed a second crystallization, to the low-temperature crystalline phase. This somewhat counter-intuitive warming sequence (i.e., amorphous to high-temperature crystalline phase to low-temperature crystalline phase) was explained with the Ostwald Step Rule, a statement that crystallization first favors the most kinetically accessible polymorph, which is not always the thermodynamically most stable phase. Hudson (2020) described a similar situation with the crystallization of two Titan nitriles, CH_3CN and C_2H_5CN, with a heavy reliance on diffraction work by Tizek et al. (2004). Two crystallization phases also were explored in our studies (Hudson et al., 2021) of propane (C_3H_8) and propylene (C_3H_6), as well as our work on $HC(O)CH_3$, acetaldehyde (Hudson and Ferrante, 2020).

We suggest that a similar situation also exists with ethylene oxide. The transition first seen on warming the amorphous ice to 75 K could be to a high-temperature crystalline phase, which is only metastable at 75 K. A second solid-solid transition, on additional warming, converts the metastable form into the thermodynamically stable low-temperature phase at 100 K. Support for this order comes from the fact that the crystalline ice formed at 75 K converted into the second crystalline phase at 100 K, but the change was irreversible (i.e., recooling never regenerated the metastable polymorph seen at 75 K).

Against this suggestion is the fact that only one form of crystalline ethylene oxide has been reported in diffraction studies at 100 and 150 K (Luger et al., 1986; Grabowsky et al., 2008). We also are not aware of any calorimetric evidence for two crystalline phases (Giauque and Gordon, 1949). A counter-argument is that the ethylene oxide solids used for the calorimetric and diffraction studies were made by cooling liquid ethylene oxide, and so a crystalline phase that is stable only in a narrow region near the compound's melting point (161 K) might have been missed. Moreover, it is perhaps not surprising that ethylene oxide would show IR evidence of two crystalline phases, as a related compound, propylene oxide, does as well. (Hudson et al., 2017a).

Table 9
IR intensities of ethylene oxide in the gas phase and as an amorphous ice.

c-C_2H_4O - Gas[a]		*c*-C_2H_4O - Amorphous Ice[b]		
Position/ cm^{-1}	A' / 10^{-18} cm $molecule^{-1}$	Position/ cm^{-1}	A' / 10^{-18} cm $molecule^{-1}$	% Change, Gas to Ice
3065	6.02	3072	1.40	−77
2978	7.36	3000	1.91	−74
1497 & 1470	0.23	1466	0.80	250
1270	2.19	1266	3.37	54
877	10.62	858	13.40	26
822 & 808	1.46	795	1.85	27

[a] Nakanaga (1981).
[b] This work. See Table 6 and the text for details.

4.3. Spectral intensities

The IR intensities of cyclopropane and ethylene oxide in the gas phase, but not the solid phase, have been studied by earlier workers, and it is of interest to see how the gas-phase literature results compare to what we are reporting here. Our comparisons are to the amorphous-ice band strengths in Tables 5 and 6, and some comparisons are in Tables 8 and 9.

Both Levin and Pearce (1978) and Kondo et al. (1979) reported IR intensities for cyclopropane gas, and there is good agreement between the results from the two groups. However, their gas-phase values differ by about 20 to 200% from our five mid-IR solid-phase band strengths in Table 5, and the direction of the variation is not easy to rationalize. See Table 8. We do not recommend using the gas-phase band strengths of cyclopropane for work with cyclopropane-containing ices unless errors of ~20% and larger can be accepted.

The situation with ethylene oxide is similar. Nakanaga (1981) published IR intensity measurements for ethylene oxide gas, and while his results agree well with expectations from high-level calculations by Puzzarini et al. (2014), they differ from our solid-phase values by about 25 to 250% for the regions he studied, as seen in Table 9. When only ethylene oxide's strongest IR feature is examined, as opposed to the broader IR regions listed by Nakanaga, the results are Nakanaga's gas-phase value of $A'(877\ cm^{-1}) = 1.06 \times 10^{-17}$ cm $molecule^{-1}$ compared to our solid-phase value of $A'(858\ cm^{-1}) = 1.34 \times 10^{-17}$ cm $molecule^{-1}$. In short, the measured gas-phase value must be raised by ~27% to match the measured solid-phase result.

We note that the two previous laboratory investigations (Bennett et al., 2005; Bergner et al., 2019) of ices containing ethylene oxide adopted a gas-phase or calculated band strength near 858 cm^{-1} that is now found to be 20–30% different from measured solid-phase values, although this difference probably is not enough to alter any qualitative conclusions in those two papers. Much greater differences exist in the literature, as described in our Introduction. The increases we have found for band strengths of both ethylene oxide and cyclopropane near 860 cm^{-1} will lead to decreases in calculated abundances of those two molecules in ices, when based on spectral measurements with that IR band.

The primary concern of this paper is quantitative measurement of IR intensities, but there exists a qualitative check on our results. The survey spectra of Figs. 2 and 5 are for ices of about the same thickness. Moreover, Table 2 shows that amorphous cyclopropane and amorphous ethylene oxide have comparable densities. Therefore, since these compounds' molar masses differ by <5% then the IR spectra of Figs. 2 and 5 are for measurements of ices with essentially the same column density (e.g., molecules cm^{-2}) along the IR path length through each ice. Looking first at the 3000 cm^{-1} region for C—H stretching vibrations for the two amorphous solids, one sees much taller peaks for cyclopropane (6C—H bonds) than for ethylene oxide (4C—H bonds), as expected. The same is true for the crystalline solids. In contrast, the region of ring deformations, around 1000 cm^{-1}, shows stronger features for ethylene

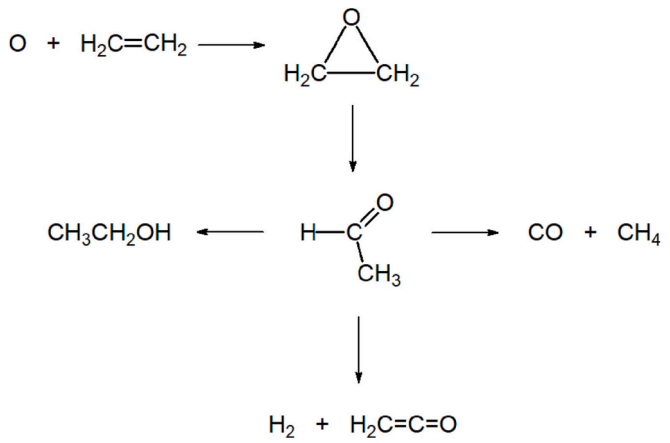

Fig. 10. Formation and subsequent reactions of ethylene oxide.

oxide than for cyclopropane, again as expected since ethylene oxide has a dipole moment, but cyclopropane does not, changes in dipole moment during a vibration being correlated with IR spectral intensity.

4.4. Applications and extensions

Applications and extensions of our work are readily envisioned. First, the optical constants $n(\tilde{\nu})$ and $k(\tilde{\nu})$ that we have calculated can be used to compute IR spectra for ices of various thicknesses. Swanepoel (1983) and Tomlin (1968) have published straightforward algebraic relations for calculating transmission and reflection spectra. Our optical constants could be particularly useful for simulating and quantifying ethylene oxide spectra obtained in a reflection mode, such as by Schriver et al. (2004) or Bennett et al. (2005). In each case, the transmission or reflection calculations will require our optical constants.

A second use of our work is as reference measurements (i.e., anchor points) for IR features we have not measured or tabulated. Our Tables 5 and 6 give IR intensities from about 4500 to 800 cm^{-1}. Infrared features in both higher- and lower-wavenumber regions could be scaled against these to determine IR intensities of near- and far-IR bands. See Gerakines et al. (2005) and Giulano et al. (2014) for examples.

A third application comes from our recent work with binary mixtures that are rich in H_2O-ice (Yarnall and Hudson, 2022b). We recently have described how data on individual compounds, such as the two considered here, can be used to obtain accurate IR band strengths for the same compounds when embedded in H_2O-ice. The same method could be applied to cyclopropane and ethylene oxide. Based on our results with benzene (C_6H_6), HCN, OCS, H_2S, and SO_2, we expect that the band strengths of the stronger IR features of ethylene oxide, a polar molecule, will hardly change if the compound is mixed with H_2O-ice. No prediction can be made at this time for cyclopropane, a non-polar molecule. A clathrate hydrate can be made with both cyclopropane and ethylene oxide (e.g., Bertie and Othen,1972; Bertie et al., 1975), but the resulting ice's band positions do not appear to differ greatly from those of each of those two compounds. For example, the well-defined peak of crystalline ethylene oxide near 1265 cm^{-1} shifts only to about 1268 cm^{-1} in the clathrate, with both ices at 100 K (Bertie and Jacobs, 1977). We have not found any published measurements of IR intensities of the clathrates to compare to the band strengths reported here.

Turning to reaction chemistry, a strong commonality exists between cyclopropane and ethylene oxide in terms of their formation at low temperatures and their destruction paths. Fig. 10 shows O-atom addition across the double bond of ethylene (C_2H_4) to make ethylene oxide. This reaction has been studied in the solid state by several research groups such as with the UV photolysis of O_3 and C_2H_4 (Hawkins and Andrews, 1983), the electron radiolysis of CO_2 and C_2H_4 (Bennett et al., 2005), and the UV photolysis of CO_2 and C_2H_4 (Bergner et al., 2019). The ethylene oxide formed will subsequently undergo ring opening to give acetaldehyde (Schriver et al., 2004), which can be reduced to ethanol (CH_3CH_2OH) or can decompose to give the other molecules shown, such as ketene, $H_2C{=}C{=}O$. See Hudson and Loeffler (2013) and references therein for ketene as a gateway to acetamide, methyl acetate, and other cometary and interstellar molecules.

An examination of Fig. 11 shows that the reactions of Fig. 10 also apply when CH_2 (methylene) combines with C_2H_4. Cyclopropane is formed, followed by reduction of the double bond to give propane ($CH_3CH_2CH_3$) or the multiple decomposition products shown. As methyl acetylene ($HC \equiv C\text{-}CH_3$) and allene ($H_2C{=}C{=}CH_2$) are among them, then

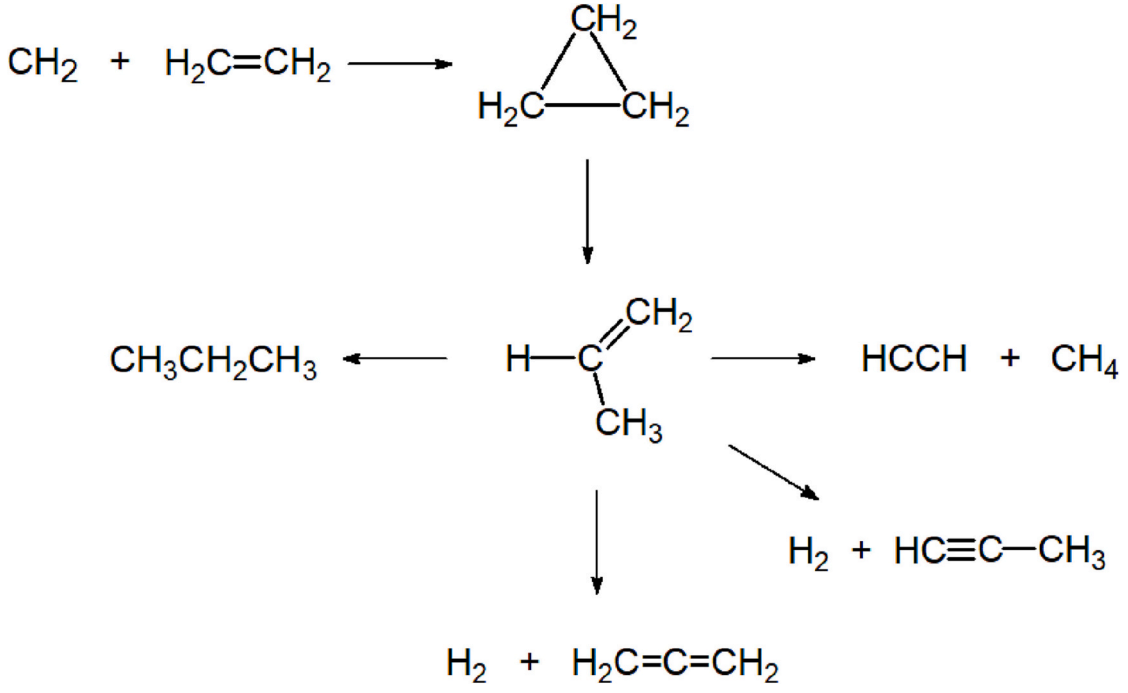

Fig. 11. Formation and subsequent reactions of cyclopropane.

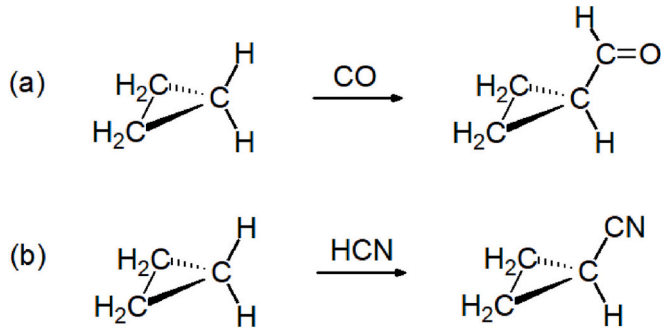

Fig. 12. Two suggested reactions from cyclopropane (non-polar) to cyclopropane derivatives (polar). Cyclopropanecarboxaldehyde is made in (a), cyclopropyl cyanide in (b). The bonds represented by heavy wedges are coming out of the plane of the figure and toward the viewer, and the bonds represented by dashed wedges are going behind the plane of the figure.

cyclopropane formation can be seen as an intermediate to lengthen carbon chains. These reactions have not been studied in the solid state to the degree that those of Fig. 10 have, probably because of the greater difficulty and danger of making CH_2 than of making O atoms. Danger and difficulty aside, CH_2 formation can be expected in extraterrestrial environments that are rich in methane (CH_4) and that are subjected to ionizing radiation, such as Titan's atmosphere and regions of Pluto, making those same environments home to the chemical changes of Fig. 11. Finally, as mentioned in our Introduction, methyl acetylene (HC ≡ C-CH_3) and allene (H_2C=C=CH_2) have been shown to undergo photolytic decomposition to make C_3, a cometary molecule, adding to the importance of understanding the formation and destruction of cyclopropane.

Concerning astronomical observations, we return to the fact that ethylene oxide and cyclopropane molecules differ in that the first is polar and the second is not. This means that remote detections of gas-phase cyclopropane are likely to be done with high-resolution IR methods, hardly a new conclusion. However, we also point out that radiolytic or photolytic reactions of cyclopropane with CO and HCN, common components of interstellar and cometary ices, should generate cyclopropanecarboxaldehyde and cyclopropyl cyanide, both polar and detectable by radio-astronomical methods. See Fig. 12. Such reaction products could be a way of identifying stable three-membered hydrocarbon rings, just as benzene (non-polar) was implicated by the identification of benzonitrile, C_6H_5-CN (McGuire et al., 2018).

We end with a comment about the possible existence of two crystalline forms of ethylene oxide discussed in Section 4.2. Although we described the IR spectra at the two higher temperatures of Fig. 6 in terms of two different phases, we recall Hirschfeld's vivid recommendation that "look like" arguments "should be terminated with extreme prejudice" (Hirschfeld, 1987). Therefore, we encourage diffraction studies and closed-cell IR measurements to produce new evidence for or against two crystalline phases of ethylene oxide. A density of the metastable form, such as from diffraction measurements, would be valuable in the calculation of that polymorph's IR intensities.

5. Summary and conclusions

The first solid-phase IR measurements of absorption coefficients, band strengths, and optical constants have been completed for amorphous and crystalline cyclopropane and ethylene oxide. Results have been compared to earlier work where possible, primarily in regard to peak positions and spectral changes with temperature. Ethylene oxide band strengths used in two previous studies have been found to need increasing by ~25% to align them with solid-phase results.

Declaration of Competing Interest

None.

Data availability

Infrared optical constants will be posted on our website.

Acknowledgments

This work was supported by the Planetary Science Division Internal Scientist Funding Program through the Fundamental Laboratory Research (FLaRe) work package at the NASA Goddard Space Flight Center. Assistance also was provided through the Goddard Center for Astrobiology and the NASA Astrobiology Institute. YYY thanks the NASA Postdoctoral Program for her fellowship.

References

Altwegg, K., Balsiger, H., Fuselier, S.A., 2019. Cometary chemistry and the origin of icy solar system bodies: the view after Rosetta. Annu. Rev. Astron. Astrophys. 57, 113–155.
Bates, J.B., Sands, D.E., Smith, W.H., 1969. Spectra and structure of crystalline cyclopropane and cyclopropane-d_6. J. Chem. Phys. 51, 105–113.
Bennett, C.J., Osamura, Y., Lebar, M.D., Kaiser, R.I., 2005. Laboratory studies on the formation of three C_2H_4O isomers - acetaldehyde (CH_3CHO), ethylene oxide (*c*-C_2H_4O), and vinyl alcohol (CH_2CHOH) - in interstellar and cometary ices. Astrophys. J. 634, 698–711.
Bergner, J.B., Oberg, K.I., Rajappan, M., 2019. Oxygen atom reactions with C_2H_6, C_2H_4, and C_2H_2 in ices. Astrophys. J. 874 (1) (16 pages).
Bernstein, L.S., Lynch, D.K., 2009. Small carbonaceous molecules, ethylene oxide (*c*-C_2H_4O) and cyclopropenylidene (*c*-C_3H_2): sources of the unidentified infrared bands? Astrophys. J. 704, 226–239.
Bertie, J.E., Jacobs, S.M., 1977. Far infrared absorption and rotational vibrations of the guest molecules in structure I clathrate hydrates between 4.3 and 100 K. Can. J. Chem. 55, 1777–1785.
Bertie, J.E., Jacobs, S.M., 1978. Far-infrared and Raman spectra, powder x-ray diffraction, and symmetry of crystalline ethylene oxide. J. Chem. Phys. 68, 97–101.
Bertie, J.E., Othen, D.A., 1973. The infrared spectrum of ethylene oxide clathrate hydrate at 100 °K between 4000 and 360 cm^{-1}. Can. J. Chem. 51, 1159–1168.
Bertie, J.E., Bates, F.E., Hendricksen, D.K., 1975. The far infrared spectra and x-ray powder diffraction patterns of the structure I hydrates of cyclopropane and ethylene oxide at 100 °K. Can. J. Chem. 53, 71–75.
Born, M., Wolf, E., 1964. Principles of Optics, 2nd (Revised) Edition. MacMillan, New York, p. 87.
Boswell, J., 1791. The Life of Samuel Johnson. Henry Baldwin, London. - See also Boswell, J., 1927. The Life of Samuel Johnson. Oxford University Press, London, p. 421 entry for 1770.
Brecher, C., Krikorian, E., Banc, J., Halford, R.S., 1961. Motions of molecules in condensed systems. X. The infrared spectrum and structure of a single crystal of cyclopropane. J. Chem. Phys. 35, 1097–1108.
Cant, N.W., Armstead, W.J., 1975. Vibrational assignment and force-field calculations for ethylene oxide. Spectrochim. Acta 31A, 839–853.
Cataliotti, R., Paliani, G., 1982. Phonon spectra and structure of crystalline ethylene oxide and ethylene sulphide at 77 K. Chem. Phys. 72, 293–300.
Coll, P., Bernard, J.-M., Navarro-González, R., Raulin, F., 2003. Oxirane: an exotic oxygenated organic compound on Titan? Astrophys. J. 598, 700–703.
DeMore, W.B., Pritchard, H.O., Davidson, N., 1959. Photochemical experiments in rigid media at low temperatures. II. The reactions of methylene, cyclopenta-dienylene and diphenylmethylene. J. Am. Chem. Soc. 81, 5874–5879.
Dickens, J.E., Irvine, W.M., Ohishi, M., Ikeda, M., Ishikawa, S., Nummelin, A., Hjarlmarson, A., 1997. Detection of interstellar ethylene oxide (*c*-C_2H_4O). Astrophys. J. 489, 753–757.
Doering, W.V.E., Zhao, D., 1995. Gas-phase addition of [13C]methylene to ethene: rearrangement of chemically excited propene. J. Am. Chem. Soc. 117, 3432–3437.
Duncan, J.L., McKean, D.C., 1968. The infrared spectrum of cyclopropane. Vapor phase and solid state spectra and assignments of cyclopropane-H_6 and -D_6. J. Mol. Spec. 27, 117–142.
Frey, H.M., 1957. Formation of cyclopropane from methylene and ethylene. J. Am. Chem. Soc. 79, 1259–1260.
Gerakines, P.A., Hudson, R.L., 2015a. The infrared spectra and optical constants of elusive amorphous methane. Astrophys. J. 805, L20–L24.
Gerakines, P.A., Hudson, R.L., 2015b. First infrared band strengths for amorphous CO_2, an overlooked component of interstellar ices. Astrophys. J. 808, L40–L46.
Gerakines, P.A., Hudson, R.L., 2020. A modified algorithm and open-source computational package for the determination of infrared optical constants relevant to astrophysics. Astrophys. J. 901, 1 (10 pages).
Gerakines, P.A., Bray, J.J., Davis, A., Richey, C., 2005. The strengths of near-infrared absorption features relevant to interstellar and planetary ices. Astrophys. J. 620, 1140–1150.

Gerakines, P.A., Yarnall, Y.Y., Hudson, R.L., 2022. Direct measurements of infrared intensities of HCN and H_2O + HCN ices for laboratory and observational astrochemistry. MNRAS 509, 3515–3522.
Giauque, W.F., Gordon, J., 1949. The entropy of ethylene oxide. Heat capacity from 14 to 285 °K. vapor pressure. Heats of fusion and vaporization. J. Am. Chem. Soc. 71, 2176–2181.
Giulano, B.M., Escribano, R.M., Martin-Doménech, R., Dartois Muñoz Caro, G.M., 2014. Interstellar ice analogs: band strengths of H_2O, CO_2, CH_3OH, and NH_3 in the far-infrared region. Astron. Astrophys. 565 (A108) (7 pages).
Grabowsky, S., Weber, M., Buschmann, J., Luger, P., 2008. Experimental electron density study of ethylene oxide at 100 K. Acta Cryst B64, 397–400.
Grundy, W.M., Binzel, R.P., Buratti, B.J., et al., 2016. Surface compositions across Pluto and Charon. Science 351 (1) (8 pages).
Hawkins, M., Andrews, L., 1983. Reactions of atomic oxygen with ethene in solid argon. J. Am. Chem. Soc. 105, 2523–2530.
Helbert, J., Rauer, H., Boice, D.C., Huebner, W.F., 2005. The chemistry of C_2 and C_3 in the coma of comet C/1995 O1 (Hale Bopp) at heliocentric distances $r_h \geq 2.9$ AU. Astron. Astrophys. 442, 1107–1120.
Herzberg, G., 1945. Molecular Spectra and Molecular Structure II. Infrared and Raman Spectra of Polyatomic Molecules. D. Van Nostrand Co, Princeton, New Jersey, USA, p. 351.
Hesman, B., Bjoraker, G.L., Sada, P.V., et al., 2012. Elusive ethylene detected in Saturn's northern storm region. Astrophys. J. 760, 1 (7 pages).
Hirschfeld, T., 1987. Computerized infrared: The need for caution. In: McClure, G.L. (Ed.), Computerized Quantitative Infrared Analysis, pp. 169–179. ASTM Special Technical Publication 934, Philadelphia, Pennsylvania, USA.
Hollenberg, J.L., Dows, D.A., 1961. Measurement of absolute infrared absorption intensities in crystals. J. Chem. Phys. 34, 1061–1063.
Hudson, R.L., 2020. Preparation, identification, and low-temperature infrared spectra of two elusive crystalline nitrile ices. Icarus 338 (1) (9 pages).
Hudson, R.L., Ferrante, R.F., 2020. Quantifying acetaldehyde in astronomical ices and laboratory analogues: IR spectra, intensities, ^{13}C shifts, and radiation chemistry. MNRAS 492, 283–293.
Hudson, R.L., Loeffler, M.J., 2013. Ketene formation in interstellar ices: a laboratory study. Astrophys. J. 773, 773–782.
Hudson, R.L., Yarnall, Y.Y., 2022a. Infrared spectra and optical constants of astronomical ices: IV. Benzene and pyridine. Icarus 377 (1) (9 pages).
Hudson, R.L., Yarnall, Y.Y., 2022b. Infrared spectra and intensities of amorphous and crystalline allene. ACS Earth Space Chem. 6, 1163–1170.
Hudson, R.L., Ferrante, R.F., Moore, M.H., 2014a. Infrared spectra and optical constants of astronomical ices: I. Amorphous and crystalline acetylene. Icarus 228, 276–287.
Hudson, R.L., Gerakines, P.A., Moore, M.H., 2014b. Infrared spectra and optical constants of astronomical ices: II. Ethane and ethylene. Icarus 243, 148–147.
Hudson, R.L., Loeffler, M.J., Yocum, K.M., 2017a. Laboratory investigations into the spectra and origin of propylene oxide, a chiral interstellar molecule. Astrophys. J. 835 (1) (9 pages).
Hudson, R.L., Loeffler, M.J., Gerakines, P.A., 2017b. Infrared spectra and band strengths of amorphous and crystalline N_2O. J. Chem. Phys. 146, 0243304.
Hudson, R.L., Gerakines, P.A., Ferrante, R.F., 2018. IR spectra and properties of solid acetone, an interstellar and cometary molecule. Spectrochim. Acta 193, 33–39.
Hudson, R.L., Loeffler, M.J., Ferrante, R.F., Gerakines, P.A., Coleman, F.M., 2020. Testing densities and refractive indices of extraterrestrial ice components using molecular structures - organic compounds and molar refractions. Astrophys. J. 891, 1 (10 pages).
Hudson, R.L., Yarnall, Y.Y., Gerakines, P.A., Coones, R.T., 2021. Infrared spectra and optical constants of astronomical ices: III. Propane, propylene, and propyne. Icarus 354, 114033 (10 pages).
Hudson, R.L., Gerakines, P.A., Yarnall, Y.Y., 2022. Ammonia ices revisited: new IR intensities and optical constants for solid NH_3. Astrophys. J. 925 (1) (8 pages).
Irvin, J.A., Quickenden, T.I., 1983. Linear least squares treatment when there are errors in both x and y. J. Chem. Educ. 60, 711–712.
Jacox, M.E., 1962. Solid-state vibrational spectra of ethylene and ethylene-d_4. J. Chem. Phys. 36, 140–143.
Jacox, M.E., Milligan, D.E., 1974. Matrix isolation study of the vacuum ultraviolet photolysis of allene and methylacetylene. Vibrational and electronic spectra of the species C_3, C_3H, C_3H_2, and C_3H_3. Chem. Phys. 4, 45–61.
Keeports, D.D., Eggers, D.F., 1986. Internal vibrational modes and intermolecular force constants in solid cyclopropane. J. Mol. Struct. 144, 11–24.
Kondo, S., Nakanaga, T., Saëki, S., 1979. Study on the i.r. band intensities of cyclopropane. Spectrochim. Acta 35A, 181–191.
Kragh, H., 2018. The Lorenz-Lorentz formula: origin and early history. Substantia 2, 7–18.
Levin, I.W., Pearce, R.A.R., 1978. Absolute infrared intensities of cyclopropane-d_0 and cyclopropane-d_6: dipole moment derivatives and polar tensors. J. Chem. Phys. 69, 2196–2208.
Linnnett, J.W., 1938. Infra-red and Raman spectra of polyatomic molecules. V. Cyclopropane and ethylene oxide. J. Chem. Phys. 6, 692–702.
Luger, P., Zaki, C., Buschmann, J., Rudert, R., 1986. Ethylene oxide x-ray structure analysis (at 150 K) and ab initio calculations. Angew. Chem. Int. Engl. Ed. 25, 276–277.
Luna, R., Satorre, M.Á., Domingo, M., Millán, C., Santonja, C., 2012. Density and refractive index of binary CH_4, N_2 and CO_2 ice mixtures. Icarus 221, 186–191.
McGuire, B.A., Burkhardt, A.M., Kalenskii, S., Shingledecker, C.N., Remijan, A.J., Herbst, E., McCarthy, M.C., 2018. Detection of the aromatic molecule benzonitrile (c-C_6H_5CN) in the interstellar medium. Science 359, 202–205.
Nakanaga, T., 1981. Infrared band intensities of ethylene oxide. J. Chem. Phys. 74, 5384–5392.
Navarro-González, R., Ramírez, S.I., 1997. Corona discharge of Titan's troposphere. Adv. Space Res. 19, 1121–1133.
Nixon, C.A., Jennings, D.E., Bezard, B.E., et al., 2014. Titan's hydrocarbon zoo: Detection of propene and the search for structural isomers. In: American Astronomical Society. DPS meeting #46, id.211.08.
Pacansky, J., England, C.D., 1986. Analysis of infrared specular reflection spectroscopy for rare gas matrices. J. Phys. Chem. 90, 4499–4508.
Press, W.H., Teukolsky, S.A., Vetterline, W.T., Flannery, B.P., 1992. Numerical Recipes in FORTRAN, 2nd edition. Cambridge Univ. Press, p. 660.
Puzzarini, C., Biczysko, M., Bloino, J., Barone, V., 2014. Accurate spectroscopic characterization of oxirane: a valuable route to its identification in Titan's atmosphere and the assignment of unidentified infrared bands. Astrophys. J. 785 (1) (8 pages).
Roush, T., 2001. Physical state of ices in the outer solar system. J. Geophys. Res. 106, 33,315–33,323.
Ruehrwein, R.A., Powell, T.M., 1946. The heat capacity, vapor pressure, heats of fusion and vaporization of cyclopropane. Entropy and density of the gas. J. Am. Chem. Soc. 68, 1063–1066.
Schriver, A., Coanga, J.M., Schriver-Mazzuoli, L., Ehrenfreund, P., 2004. Vibrational spectra and UV photochemistry of $(CH_3)_2O$ thin films and $(CH_3)_2O$ in amorphous water ice. Chem. Phys. 303, 13–25.
Shimanouchi, T., 1972. Tables of Molecular Vibrational Frequencies Consolidated Volume 1, United States Department of Commerce, National Bureau of Standards, NSRDS-NBS 39. US Government Printing Office, Washington, DC, USA.
Stief, L.J., 1972. Origin of C_3 in comets. Nature 237, 92.
Swanepoel, R., 1983. Determination of the thickness and optical constants of amorphous silicon. J. Phys. E: Sci. Instrum. 16, 1214–1222.
Tempelmeyer, K.E., Mills, D.W., 1968. Refractive index of carbon dioxide cryodeposit. J. Appl. Phys. 39, 2968–2969.
Thakkar, A.J., Wu, T., 2015. How well do static electronic dipole polarizabilities from gas-phase experiments compare with density functional and MP2 calculations? J. Chem. Phys. 143, 144302 (8 pages).
Tizek, H., Grothe, H., Knozinger, E., 2004. Gas-phase deposition of acetonitrile: an attempt to understand Ostwald's step rule on a molecular basis. Chem. Phys. Lett. 383, 129–133.
Tomlin, S.G., 1968. Optical transmission and reflection formulae for thin films. Br. J. Appl. Phys. (J. Phys. D) 2, 1667–1671.
Ward, M.D., Price, S.D., 2011. Thermal reaction of oxygen atoms with alkenes at low temperature on interstellar dust. Astrophys. J. 741 (1) (9 pages).
Weiler, M., 2012. The chemistry of C3 and C2 in cometary comae. I. Current models revisited. A&A 538 (A149) (12 pages).
Yarnall, Y.Y., Hudson, R.L., 2022a. Crystalline ices – densities and comparisons for planetary and interstellar applications. Icarus 373 (1) (4 pages).
Yarnall, Y.Y., Hudson, R.L., 2022b. A new method for measuring IR band strengths in H_2O-ices: first results for OCS, H_2S, and SO_2. Astrophys. J. 91 (L4) (6 pages).